nature chemical biology

ARTICLES

https://doi.org/10.1038/s41589-019-0392-5

Site-specific acylation of a bacterial virulence regulator attenuates infection

Zhenrun J. Zhang[1], Virginia A. Pedicord[1,2], Tao Peng[1,3] and Howard C. Hang[1*]

Microbiota generates millimolar concentrations of short-chain fatty acids (SCFAs) that can modulate host metabolism, immunity and susceptibility to infection. Butyrate in particular can function as a carbon source and anti-inflammatory metabolite, but the mechanism by which it inhibits pathogen virulence has been elusive. Using chemical proteomics, we found that several virulence factors encoded by *Salmonella* pathogenicity island-1 (SPI-1) are acylated by SCFAs. Notably, a transcriptional regulator of SPI-1, HilA, was acylated on several key lysine residues. Subsequent incorporation of stable butyryl-lysine analogs using CRISPR–Cas9 gene editing and unnatural amino acid mutagenesis revealed that site-specific modification of HilA impacts its genomic occupancy, expression of SPI-1 genes and attenuates *Salmonella enterica* serovar Typhimurium invasion of epithelial cells, as well as dissemination in vivo. Moreover, a multiple-site HilA lysine acylation mutant strain of *S.* Typhimurium was resistant to butyrate inhibition ex vivo and microbiota attenuation in vivo. Our results suggest that prominent microbiota-derived metabolites may directly acylate virulence factors to inhibit microbial pathogenesis in vivo.

Short-chain fatty acids generated by gut microbiota fermentation of dietary polysaccharides exhibit substantial effects on host physiology and immunity[1]. SCFA concentrations in the mammalian gut range from 1–100 mM (ref. [2]), depending on the location in the intestine, host diet and microbiota composition. Specific microbiota reconstitution studies have revealed that *Clostridia* cluster IV, XIVa and XVIII are key bacterial species involved in SCFA fermentation in the gut[3]. Amongst the SCFAs generated in vivo, butyrate has been reported to function as a nutrient source for colonocytes[4], and as an agonist for G protein-coupled receptors (GPR41, GPR43, GPR109A) in multiple cell types[5–9] to maintain intestinal barrier function. Moreover, butyrate has been suggested to function as a lysine deacetylase inhibitor to suppress inflammation in peripheral regulatory T (T_{reg}) cells[3,10–12], macrophages[13] and dendritic cells[7], as well as to prime an antimicrobial program in macrophages[14]. *Clostridia* cluster IV, XIVa and XVIII production of butyrate is also implicated in peroxisome proliferator-activated receptor-γ signaling to limit the lumen oxygen availability and prevent the expansion of *S.* Typhimurium in the intestinal lumen[15,16].

Beyond modulating host-signaling pathways to fortify intestinal barrier integrity and suppress inflammation, microbiota-derived butyrate can also function as a nutrient source and directly attenuate the virulence of enteric pathogens. Depletion of microbiota with broad-spectrum antibiotics or streptomycin alone increases host susceptibility to *S.* Typhimurium infection[16], which can be ameliorated by recolonization with butyrate-producing *Clostridia*[16]. Butyrate production by the microbiota has also been suggested to act as a carbon source for *S.* Typhimurium that expresses the *ydiQRSTD* operon[17]. Notably, butyrate also inhibits the expression of virulence-associated genes in the SPI-1 locus[18,19], which encodes transcriptional regulators, chaperones, secreted protein effectors and needle components of the type III secretion system required for invasion of epithelial cells and bacterial pathogenesis in vivo[20]. Nonetheless, the molecular mechanism by which butyrate directly inhibits the expression of SPI-1 virulence genes and *S.* Typhimurium infection is unclear.

To identify the protein targets of butyrate in *S.* Typhimurium, we employed a SCFA chemical reporter and label-free quantitative proteomics. We found that several virulence factors encoded within the SPI-1 locus could be acylated in *S.* Typhimurium. Amongst these acylated proteins, we focused on HilA, a key transcriptional regulator of SPI-1 gene expression and *S.* Typhimurium virulence. To address the potential site-specific functions of HilA acylation, we utilized CRISPR–Cas9 gene editing and genetic code expansion to install stable butyryl-lysine analogs at key lysine residues on chromosomally expressed HilA. Our analysis of these engineered *S.* Typhimurium strains demonstrated that site-specific butyrylation can inhibit and enhance HilA activity. Notably, acylation of lysine 90 impairs HilA occupancy and expression of SPI-1 genes, as well as attenuating *S.* Typhimurium invasion of epithelial cells and pathogenesis in vivo. Moreover, a multisite lysine-to-arginine and acylation-defective HilA mutant strain of *S.* Typhimurium was resistant to butyrate-mediated suppression of SPI-1 genes and slightly more virulent in microbiota-sufficient mice in vivo. Our results suggest that microbiota-derived SCFA acylation of key virulence factors may attenuate intestinal pathogen infection in vivo.

Results

Proteomic analysis of acylated proteins in *Salmonella*. Given that protein acylation is prevalent in bacteria[21], we explored whether microbiota-derived butyrate could acylate specific *S.* Typhimurium proteins involved in SPI-1 regulation using an alkyne butyrate analog (alk-3, pentynoate) (Supplementary Fig. 1a)[22] and chemical proteomics (Supplementary Fig. 1b)[23]. Alk-3 behaved similarly to butyrate and did not affect *S.* Typhimurium (strain 14028S) growth at 10 mM (Supplementary Fig. 1c), but inhibited expression of the SPI-1 gene *sipA* (Supplementary Fig. 1d) and *S.* Typhimurium invasion of HeLa cells (Supplementary Fig. 1e). To visualize acylated proteins, the total cell lysates from alk-3-treated *S.* Typhimurium cultures were reacted via bioorthogonal labeling with azide-Rhodamine (az-Rho) for in-gel fluorescence profiling (Supplementary Fig. 1b),

[1]Laboratory of Chemical Biology and Microbial Pathogenesis, The Rockefeller University, New York, NY, USA. [2]Cambridge Institute of Therapeutic Immunology & Infectious Disease (CITIID), Department of Medicine, University of Cambridge, Cambridge, UK. [3]State Key Laboratory of Chemical Oncogenomics, School of Chemical Biology and Biotechnology, Peking University Shenzhen Graduate School, Shenzhen, China. *e-mail: hhang@rockefeller.edu

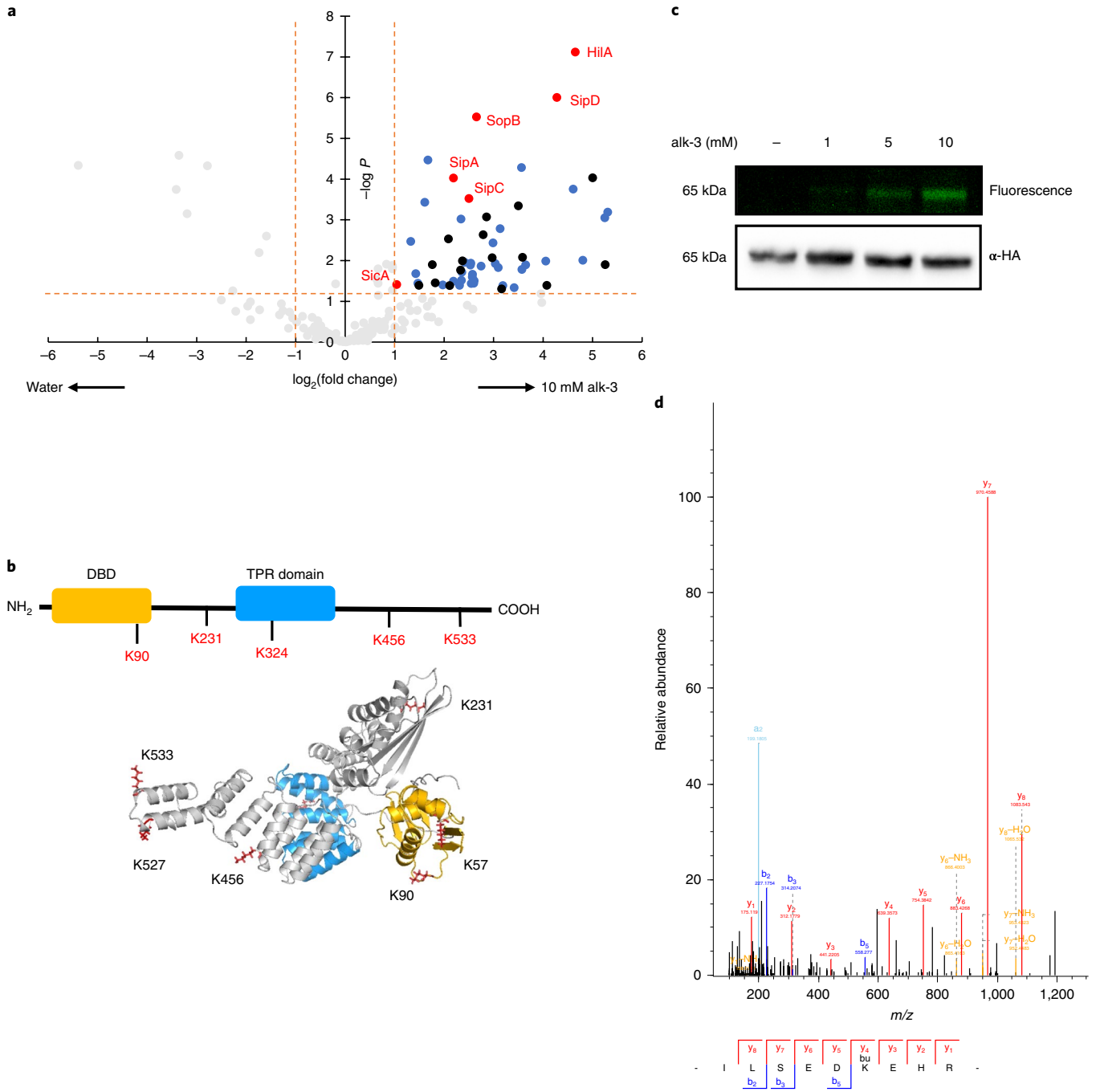


Fig. 1 | Proteomic analysis of acylated proteins in *S.* Typhimurium. a, LFQ proteomic analysis of alk-3-labeled proteins in *S.* Typhimurium ($n = 4$). *S.* Typhimurium cell lysates were reacted with az-biotin for the enrichment of alk-3-labeled proteins with streptavidin beads and identification by LC–MS/MS. Proteins that were enriched by alk-3 (top right corner) were colored according to their annotated biological function: blue, metabolic enzymes; red, SPI-1 proteins; black, other proteins. **b**, Domain architecture (top) and predicted structure of HilA (bottom). Domain architecture was assigned by NCBI Conserved Domain Search. Structure prediction was performed with Robetta. DBD, DNA-binding domain, yellow. TPR, tetratricopeptide repeat, blue. Lysine residues detected to be acylated (K90, K231, K324, K456, K533) and two additional lysine residues that serve as controls (K57, K527) are highlighted in red. K324 is buried in the back (see Supplementary Fig. 9). **c**, Alk-3 dose-dependent labeling on HilA. *S.* Typhimurium Δ*hilA* (ref. [50]) overexpressing HilA-HA-His were grown with different concentrations of alk-3 before cell lysates were reacted with az-Rho, followed by anti-HA immunoprecipitation, SDS-PAGE in-gel fluorescence scanning (top) and anti-HA immunoblotting (bottom). Also, see Supplementary Fig. 14. **d**, MS/MS spectrum of HilA K90 butyrylated (K90bu) peptide detected from HilA purified from *S.* Typhimurium grown with 10 mM butyrate.

which revealed many alk-3-modified proteins (Supplementary Fig. 1f). To identify these acylated proteins, alk-3-labeled total cell lysates were reacted with azide-biotin (az-biotin), enriched by streptavidin beads and analyzed by label-free quantitative (LFQ) proteomics. From this analysis, 56 proteins were selectively enriched more than twofold in alk-3 samples with *P* values less than 0.05 (Fig. 1a and Supplementary Dataset 1). Bioinformatic analysis of the alk-3 hits recovered several proteins involved in metabolism, as well as a few key effectors and regulators (SipD, SopB, SipA, SipC, SicA and HilA) of *S.* Typhimurium pathogenesis (Fig. 1a, Supplementary Dataset 1

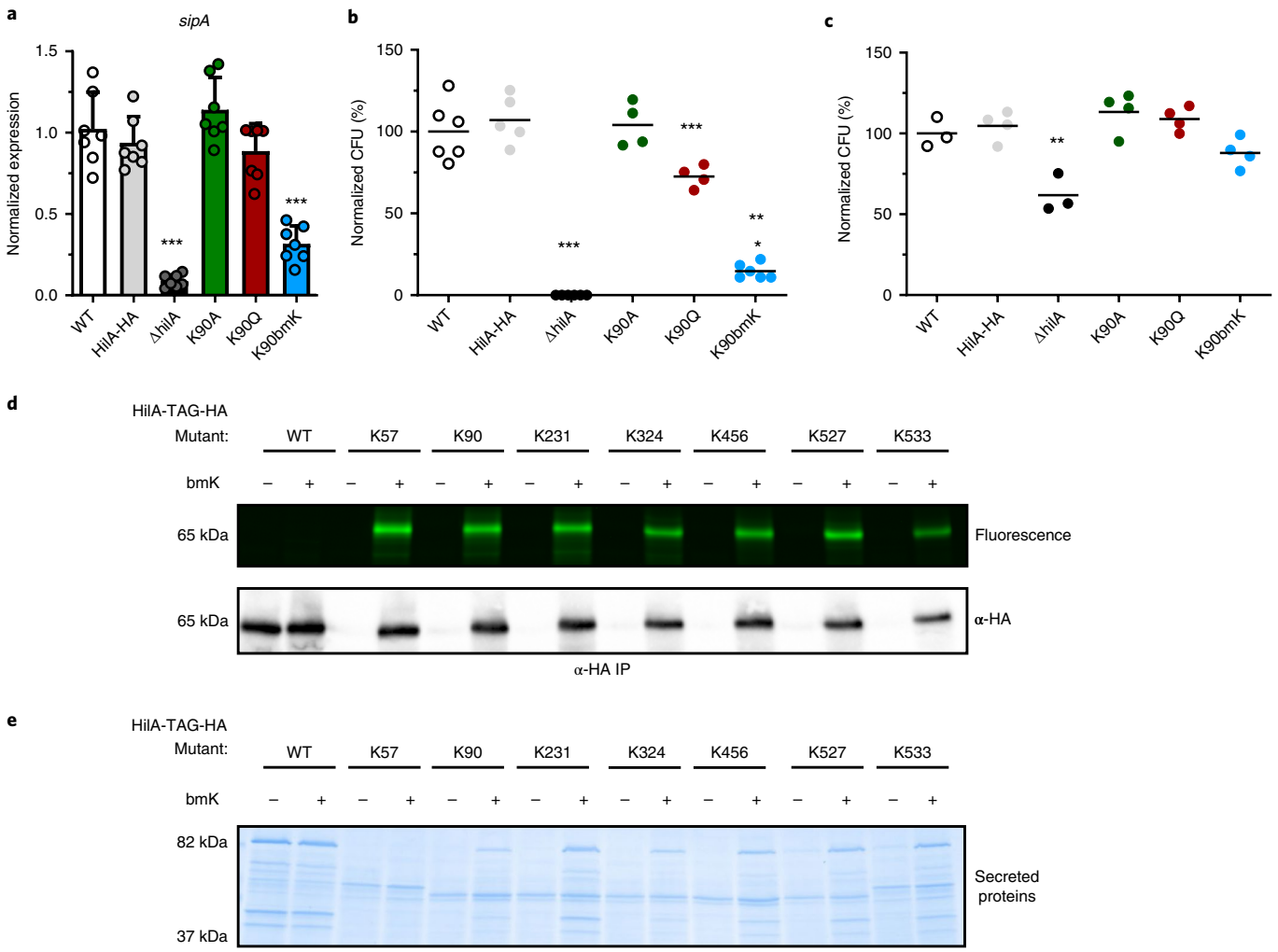


Fig. 2 | Site-specific mutation of HilA affects *S.* Typhimurium virulence. a, Relative expression level of SPI-1 gene *sipA* in *S.* Typhimurium WT, HilA-HA strain, Δ*hilA* strain, HilA-K90A-HA and HilA-K90Q-HA mutants measured by qRT–PCR ($n = 7$–8). All mutants were compared to WT with one-way ANOVA and Dunnett's post-test. Error bar, s.d. $^{**}P < 0.01$; $^{***}P < 0.001$. Comparisons with no asterisk had $P > 0.05$ and were not considered significant. **b**,**c**, Gentamicin protection assay of *S.* Typhimurium WT, HilA-HA strain, Δ*hilA* strain, HilA-K90A-HA, HilA-K90Q-HA, and HilA-K90bmK-HA mutants infecting HeLa cells (**b**) or RAW264.7 macrophages (**c**) at MOI = 10 ($n = 3$–6). All mutants were compared to HilA-HA with one-way ANOVA and Dunnett's post-test. Centerline, average. $^{**}P < 0.01$. Comparisons with no asterisk had $P > 0.05$ and were not considered significant. **d**, Endogenous expression of HilA-bmK-HA mutants in *S.* Typhimurium. *S.* Typhimurium HilA-HA strain (WT) and amber codon mutants (HilA-TAG-HA) with amber codon suppression system were grown with or without 100 μM bmK. Anti-HA immunoprecipitated (IP) samples were analyzed with SDS–PAGE in-gel fluorescence scanning (top) and anti-HA immunoblotting. Also, see Supplementary Fig. 14. **e**, Secreted proteins of *S.* Typhimurium endogenous HilA-bmK-HA mutants. *S.* Typhimurium HilA-HA strain (WT) and amber codon mutants (HilA-TAG-HA) with amber codon suppression system were grown with or without 100 μM bmK. Supernatants of the cultures were precipitated with 10% trichloroacetic acid and analyzed with SDS–PAGE Coomassie Blue staining.

and Supplementary Table 1). While the SPI-1 transcriptional regulator HilD has been suggested to modulate propionate activity in *S.* Typhimurium[24], and could be regulated by acetylation[25], it was not labeled by alk-3 in our proteomic dataset (Supplementary Dataset 1) or when overexpressed (Supplementary Fig. 2a). Of note is that HilA, a key transcriptional regulator of SPI-1 genes[26,27], was one of the most prominent acylated *S.* Typhimurium candidate proteins in the dataset (Fig. 1a and Supplementary Dataset 1).

HilA is a transcription regulator that regulates the expression of SPI-1 genes encoding type III secretion system components and substrates[26–30] and is also essential for *S.* Typhimurium infection in vitro[31] and pathogenesis in vivo[32]. HilA protein is predicted to contain an amino (N)-terminal DNA-binding domain that is homologous to the OmpR/PhoB family of transcription factors in bacteria[29], and a tetratricopeptide repeat (TPR) domain towards the carboxy (C) terminus (Fig. 1b). To characterize HilA acylation, we expressed epitope-tagged HilA-HA-His6 (HA, hemagglutinin) in *S.* Typhimurium and validated labeling with alk-3 (Supplementary Fig. 2b), which was dose dependent (Fig. 1c), resistant to hydroxylamine treatment (Supplementary Fig. 2c) and insensitive to the overexpression of *S.* Typhimurium acyltransferase YfiQ (Pat) or deacylase enzyme CobB, respectively (Supplementary Fig. 2d,e), suggesting that HilA acylation occurs through post-translational chemical acylation of lysine residues. In addition, deletion of other candidate protein acyltransferase genes (*yfiQ*, *yiaC* or *yjaB*), homologous to *Escherichia coli yiaC* and *yjaB* (ref. [33]), in *S.* Typhimurium did not affect alk-3 labeling of HilA (Supplementary Fig. 2f), further suggesting that millimolar levels of exogenous butyrate chemically acylates HilA through high-energy acyl-coenzyme A or phosphate intermediates in *S.* Typhimurium.

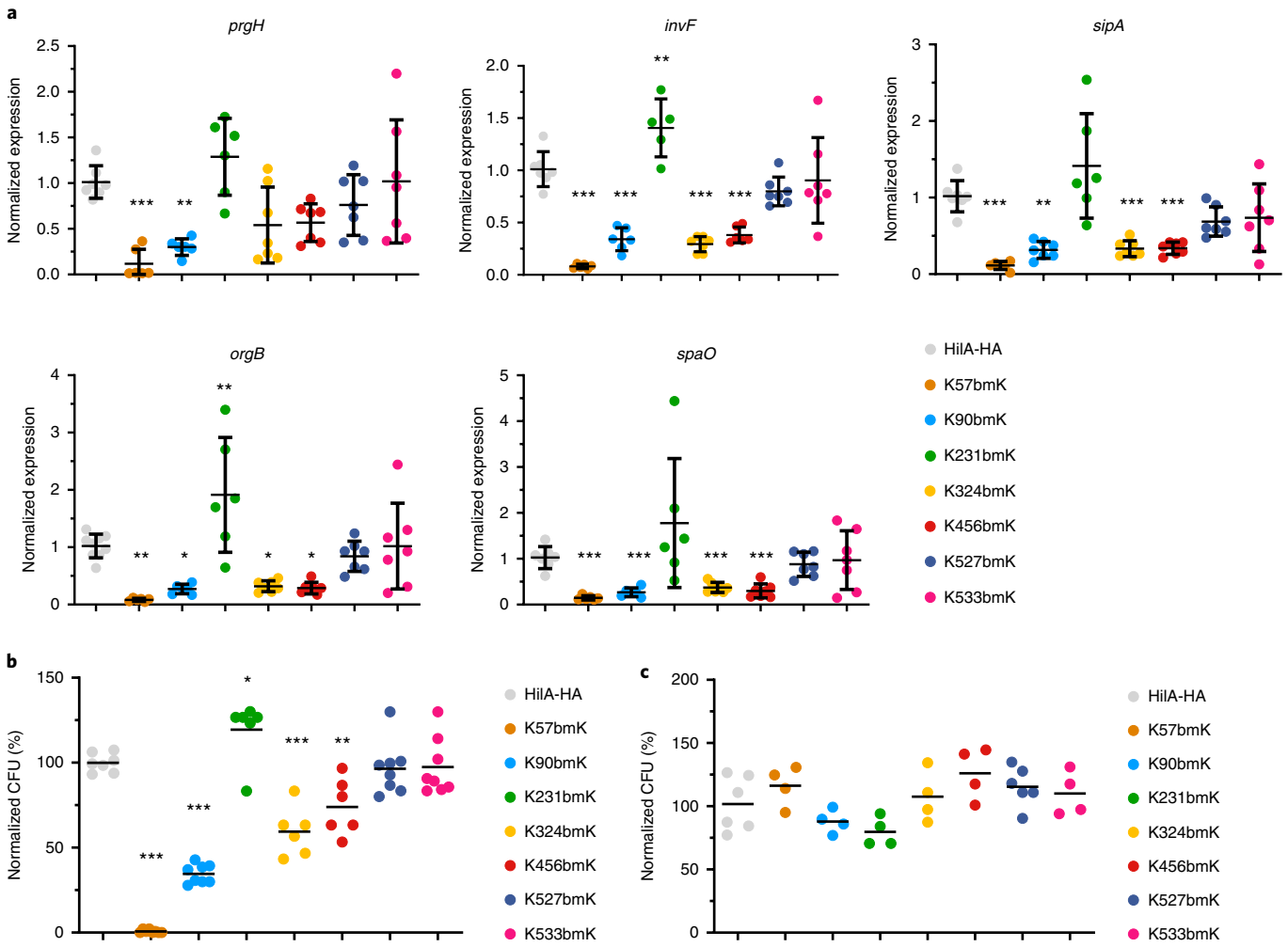


Fig. 3 | Site-specific acylation of HilA affects *S.* Typhimurium transcriptional activity and invasion in vitro. a, Relative expression level of SPI-1 genes in several operons (*prgH, invF, sipA, orgB* and *spaO*) in *S.* Typhimurium HilA-HA strains and HilA-bmK-HA mutants measured by qRT-PCR ($n = 6$–8). All mutants were compared to HilA-HA with one-way ANOVA and Dunnett's post-test. Centerline, average. Error bar, s.d. $^{*}P < 0.05$; $^{**}P < 0.01$; $^{***}P < 0.001$. Comparisons with no asterisk had $P > 0.05$ and were not considered significant. **b**,**c**, Gentamicin protection assay of *S.* Typhimurium endogenous HilA-bmK-HA mutants infecting HeLa cells (**b**) or RAW264.7 macrophages (**c**) at MOI = 10 ($n = 4$–8). All mutants were compared to HilA-HA with one-way ANOVA and Dunnett's post-test. Centerline, average. $^{*}P < 0.05$; $^{**}P < 0.01$; $^{***}P < 0.001$. Comparisons with no asterisk had $P > 0.05$ and were not considered significant.

To characterize HilA acylation, we expressed and purified HilA-HA-His6 from *S.* Typhimurium incubated with 10 mM butyrate to identify sites of acylation. Of the 34 lysine residues in HilA (Supplementary Fig. 3a), we identified five lysines (K90, K231, K324, K456 and K533) that were modified with acetate, propionate or butyrate by liquid chromatography–tandem mass spectroscopy (LC–MS/MS) analysis of tryptic peptides (Supplementary Fig. 3b–d and Supplementary Table 2), consistent with previous HilA acetylation studies[34]. Protein structure prediction of HilA by Robetta[35] suggests that all five acylated lysine residues are located at surface-exposed sites for potential chemical acylation and are in predicted DNA-binding (K90) or protein–protein (K231, K324, K456) interaction domains (Fig. 1b). Amongst the five SCFA-modified lysine residues, K90 was the most prominent acylation site when we compared the ratio of acylated and unmodified peptides (Fig. 1d and Supplementary Table 2).

Site-specific incorporation of acyl-lysine analogs into HilA. To evaluate site-specific lysine butyrylation of HilA in *S.* Typhimurium in vivo, we explored genetic code expansion with N^{ε}-butyryl-lysine analogs (Supplementary Fig. 4a)[36–38]. Expression of wild-type (WT) *Methanosarcina mazei* pyrrolysine-transfer RNA synthetase (*Mm*PylRS-WT) and $tRNA^{Pyl}_{CUA}$ in *S.* Typhimurium showed poor incorporation of N^{ε}-butyryl-lysine (buK) into overexpressed HilA-HA bearing an amber codon at K90 (HilA-K90-TAG-HA) (Supplementary Fig. 4b,c). We then evaluated other PylRS mutants with buK and other analogs for improved incorporation of potential butyryl-lysine mimics (Supplementary Fig. 4b). Analysis of HilA-HA protein levels revealed that N^{ε}-pent-4-ynyloxy-carbonyl-lysine[39] afforded near wild-type levels of HilA-K90-TAG-HA with *M. barkeri* PylRS-ASF mutant (*Mb*PylRS-ASF)[39–41] (Supplementary Fig. 4b,c), which also cross-reacted with anti-butyryl-lysine antibody (Supplementary Fig. 4c) and was readily detected by bioorthogonal labeling (Supplementary Fig. 4c). We subsequently employed this compound as a lysine butyrylation mimic (bmK) in *S.* Typhimurium.

To incorporate bmK into chromosomally expressed HilA, we optimized CRISPR–Cas9 gene editing[42] in *S.* Typhimurium using single-stranded DNA (ssDNA) templates and liquid selection (Supplementary Figs. 5 and 6). Our optimized CRISPR–Cas9

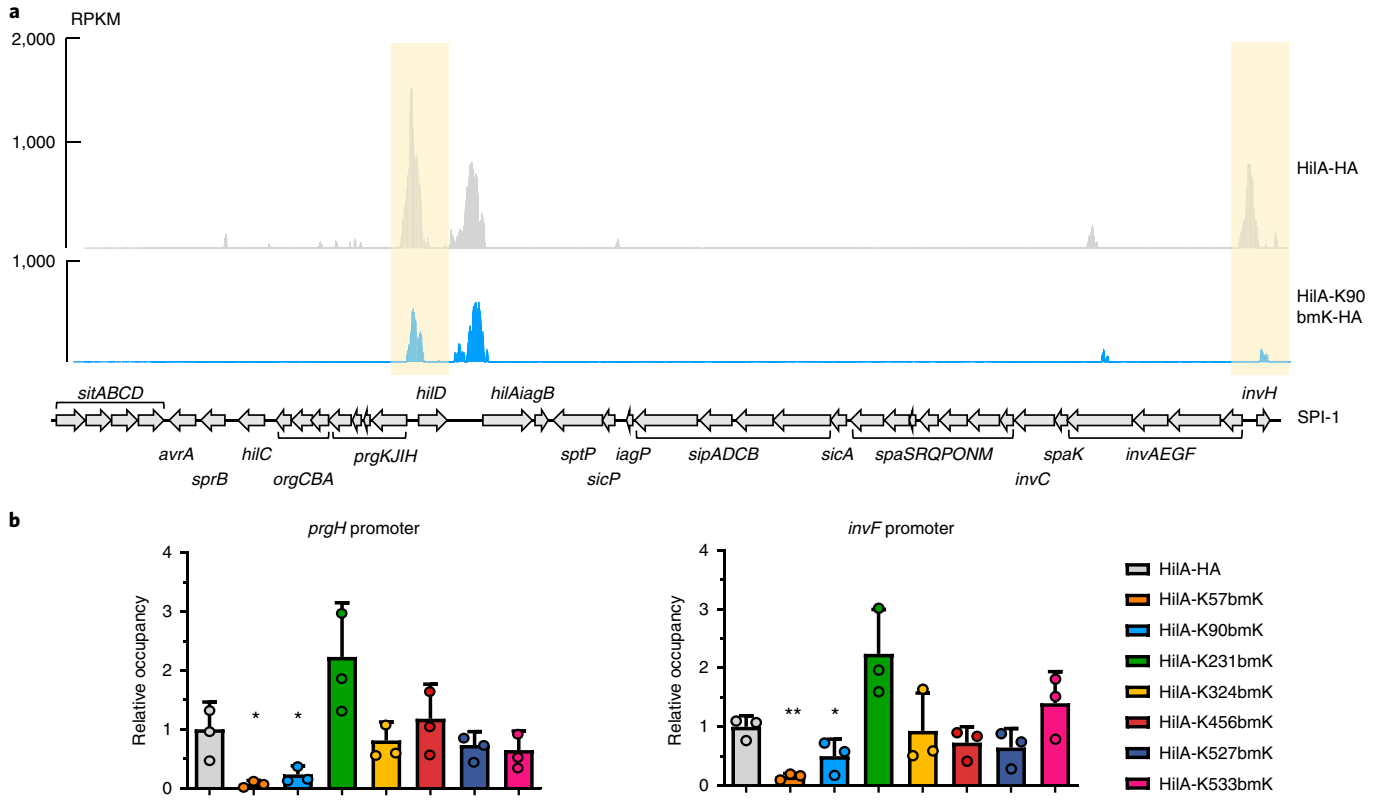


Fig. 4 | HilA K90 acylation affects its occupancy at target genes. a, Cross-link IP-seq results on *S.* Typhimurium HilA-HA and *S.* Typhimurium HilA-K90bmK-HA in the SPI-1 region. Yellow shading, *prgH* promoter region (left) and *invF* promoter region (right). RPKM, reads per kilobase million. **b**, Cross-link IP–qPCR of *prgH* promoter region (left) or *invF* promoter region (right) of *S.* Typhimurium endogenous HilA-bmK-HA mutants ($n=3$). All mutants were compared to HilA-HA with one-way ANOVA and Dunnett's post-test. Error bar, s.d. $^{*}P<0.05$; $^{**}P<0.01$. Comparisons with no asterisk had $P>0.05$ and were not considered significant.

gene-editing protocol enabled chromosomal insertion of an HA-tag at the C terminus of HilA as well as alanine, glutamine and TAG mutants at K90. The specificity of our CRISPR–Cas9 gene-editing protocol was confirmed by whole-genome sequencing of HilA-HA and HilA-K90-TAG-HA *S.* Typhimurium strains (Supplementary Table 3). The activity of the HilA-HA, K90A and K90Q (an acetylation mimic) on SPI-1 gene expression was similar to the parent *S.* Typhimurium (strain 14028S) (Fig. 2a). However, HilA-K90bmK-HA showed significant reduction of SPI-1 gene expression, almost to *ΔhilA* levels (Fig. 2a). These differences in SPI-1 gene expression were correlated with *S.* Typhimurium HilA-K90 mutant infection of HeLa cells (Fig. 2b) and were not significant in RAW264.7 macrophages (Fig. 2c), which are less dependent on SPI-1 for invasion[43]. These results demonstrate that classical site-directed mutagenesis to canonical amino acids may not reveal how site-specific metabolite modifications regulate protein function in cells.

Site-specific acylation of HilA affects *Salmonella* virulence. We then generated additional *S.* Typhimurium strains with chromosomal amber codon mutants at K231, K324, K456 and K533 in HilA-HA to evaluate site-specific differences in activity. To control for nonspecific effects of bmK incorporation into HilA, we also generated amber codon mutants at K57 and K527 that are not acylated, based on our MS/MS analysis, but that could function as controls for protein expression and activity. Importantly, these engineered HilA-HA strains replicated at similar rates to the parent *S.* Typhimurium strain 14028S in liquid culture (Supplementary Fig. 7a) and efficiently incorporated bmK into the HilA-TAG-HA mutants that were readily detected by bioorthogonal labeling and anti-HA immunoblotting (Fig. 2d). To control for genetic code expansion, the HilA-HA *S.* Typhimurium strain (WT) was also transformed with plasmid encoding PylRS and $tRNA^{CUA}$ and labeled with the same concentration of bmK for all subsequent experiments. A comparative analysis of HilA mutants showed that full-length HilA-HA expression in amber codon mutants depended on the presence of bmK (Fig. 2d and Supplementary Fig. 7c,d). BmK incorporation at K57, K90 and K527 yielded near wild-type levels of full-length protein, whereas K231, K324, K456 and K533 amber codon mutants afforded slightly lower amounts of HilA-HA (Supplementary Fig. 7b,d). Nonetheless, the analysis of these *S.* Typhimurium strains demonstrated that HilA-bmK-HA protein levels are not correlated with the levels of SPI-1 secreted proteins (Fig. 2e), suggesting site-specific effects of lysine butyrylation on HilA function.

We then evaluated the transcriptional activity of site-specifically acylated HilA mutants in *S.* Typhimurium. Quantitative PCR with reverse transcription (qRT–PCR) analysis of HilA target genes showed that, relative to WT HilA-HA, site-specific incorporation of bmK at K57, K90, K324 and K456 afforded reduced expression of *prgH, invF, sipA, orgB* and *spaO* located in different operons within the SPI-1 locus (Fig. 3a). While K57 is not acylated, it is predicted to be in the DNA-binding interface of HilA (Fig. 1c), and, on bmK incorporation, showed significantly reduced expression of HilA target genes (Fig. 3a), serving as a positive control loss-of-function HilA mutant. Interestingly, acylated K90 within the DNA-binding domain of HilA (Fig. 1c) also showed significantly reduced expression of HilA target genes with bmK incorporation (Fig. 3a). The incorporation of bmK into the TPR domain

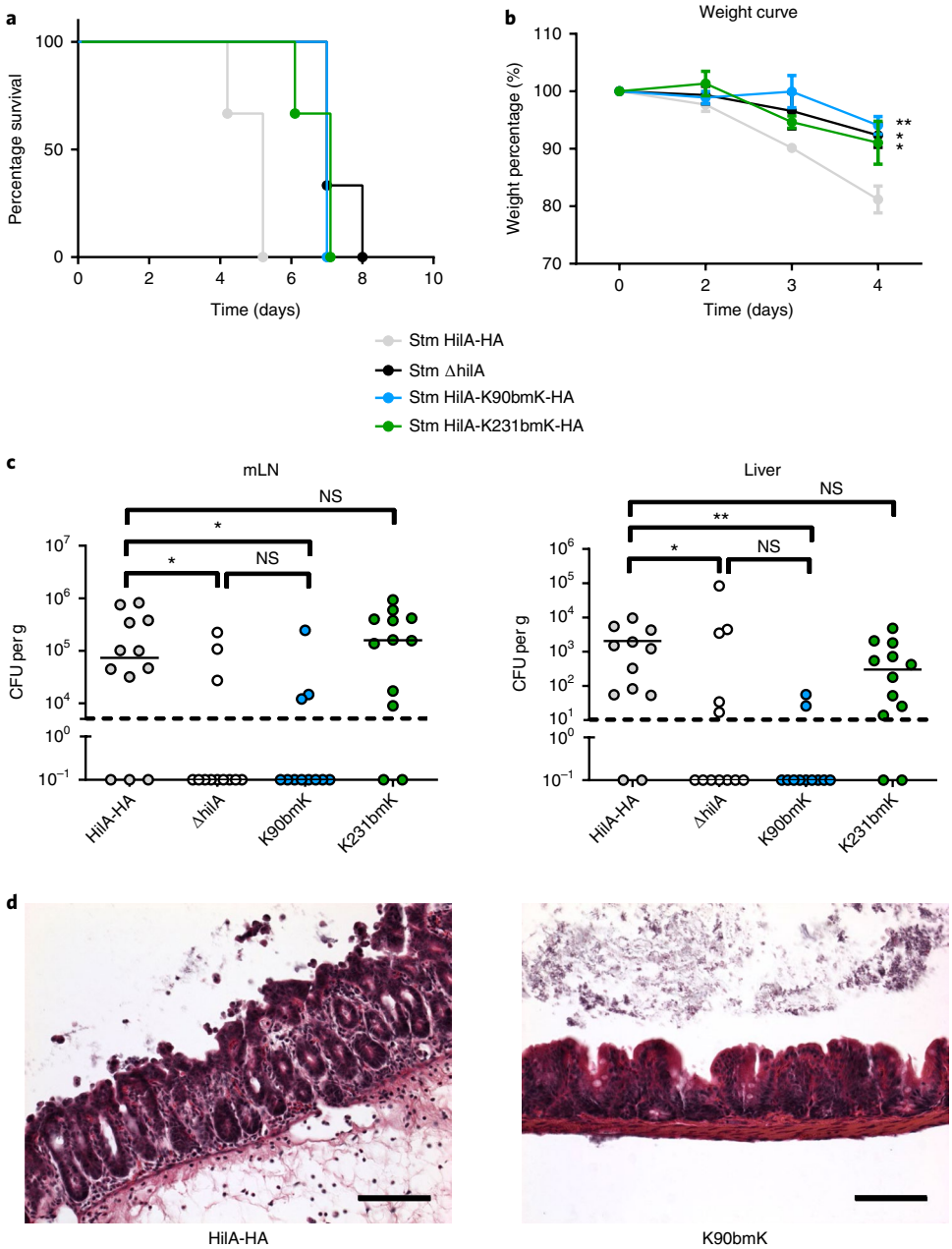


Fig. 5 | HilA K90 acylation affects *S.* Typhimurium infection and intestinal inflammation in vivo. a,**b**, C57BL/6 mice were orally infected with 10^6 CFU *S.* Typhimurium (Stm) HilA-HA strain, Δ*hilA* strain, HilA-K90bmK-HA or HilA-K231bmK-HA mutant ($n=3$). Survival (**a**) and weight loss (**b**) are shown. Weights of all mutants at day 4 were compared to HilA-HA with one-way ANOVA and Dunnett's post-test. Error bar, s.d. $^*P<0.05$; $^{**}P<0.01$. **c**, *S.* Typhimurium bacterial CFU counted from mesenteric lymph nodes (mLN, left) or liver (right) of mice orally infected with *S.* Typhimurium HilA-HA, Δ*hilA*, HilA-K90bmK-HA or HilA-K231bmK-HA at 48 h postinfection ($n=12$). HilA-K90bmK-HA and HilA-K231bmK-HA mutants were compared to HilA-HA or Δ*hilA* with Kruskal–Wallis test and Dunn's post-test. Centerline, median. $^*P<0.05$; $^{**}P<0.01$. NS, not significant. Dashed line, detection limit. **d**, Representative images of cecum tissue stained with hemotoxylin and eosin, collected 48 h postinfection from mice infected with *S.* Typhimurium HilA-HA or HilA-K90bmK-HA. Scale bar, 100 μm.

of HilA at K324 and K456 also impaired the expression of SPI-1 genes (Fig. 3a). Alternatively, bmK incorporation at K231 afforded slightly enhanced expression of HilA target genes compared to WT HilA-HA, bmK at K527 (nonacylated control for bmK incorporation) and K533 (Fig. 3a). While buK did not get incorporated into HilA-TAG-HA mutants as efficiently as bmK (Supplementary Fig. 4b), we observed similar site-specific effects on the expression of SPI-1 genes, albeit at lower levels (Supplementary Fig. 8a).

To investigate the significance of site-specific acylation of HilA on *S.* Typhimurium virulence, we analyzed the invasion of the HeLa epithelial cell line by *S.* Typhimurium. For these experiments, both wild-type and HilA mutant *S.* Typhimurium strains were transformed with PylRS and $tRNA^{CUA}$ expression plasmid, metabolically labeled with bmK, diluted with PBS buffer and used for infection. In comparison with the other lysine residues in HilA-HA, bmK incorporation at K57 (loss-of-function control), K90, K324 and K456 attenuated *S.* Typhimurium infection of HeLa cells, whereas K231 showed enhanced or similar levels of infection compared to wild-type HilA, K527 (neutral control) and K533 bmK mutants (Fig. 3b). There were no significant differences in infectivity among

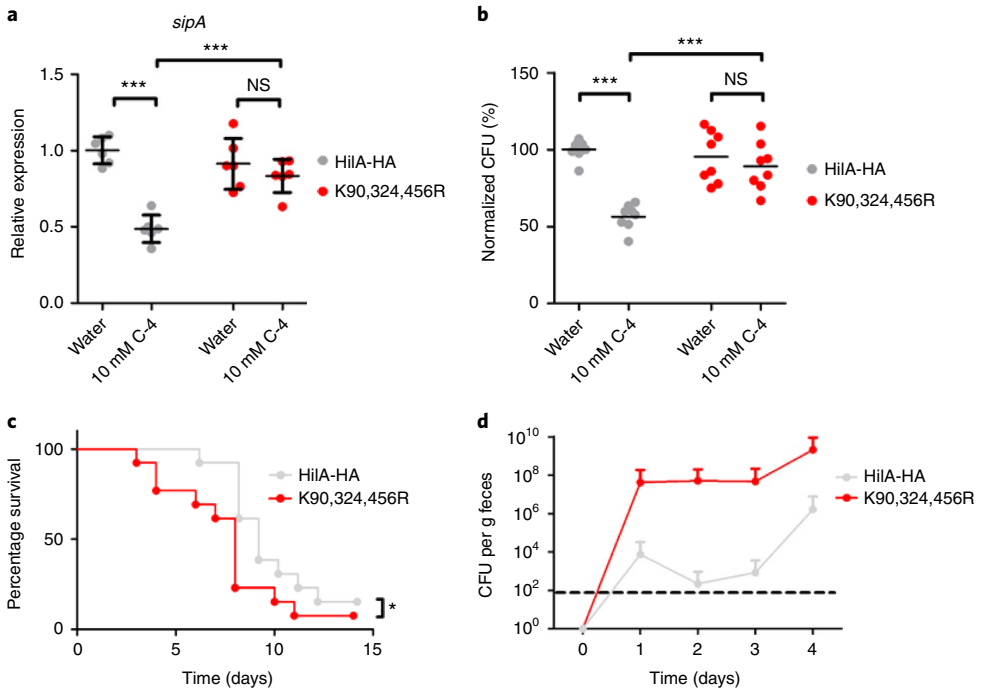


Fig. 6 | HilA-K90,324,456R mutant resists butyrate inhibition in vitro and in vivo. a, Relative expression level of SPI-1 gene *sipA* in *S.* Typhimurium HilA-HA strains and HilA-K90,324,456R-HA mutant in the presence or absence of 10 mM butyrate measured by qRT-PCR ($n = 6$). Mutants were compared with one-way ANOVA and Bonferroni post-test. Centerline, average. Error bar, s.d. ***$P < 0.001$. **b**, Gentamicin protection assay of *Salmonella* HilA-HA strains and HilA-K90,324,456R-HA mutant in the presence or absence of 10 mM butyrate infecting HeLa cells at MOI = 10 ($n = 8$). Mutants were compared with one-way ANOVA and Bonferroni post-test. Centerline, average. Error bar, s.d. ***$P < 0.001$. **c**, Survival curve of C57BL/6 mice orally infected with 10^6 CFU *S.* Typhimurium HilA-HA or K90,324,456 R mutant ($n = 13$). Groups were compared with the Gehan–Breslow–Wilcoxon test. *$P < 0.05$. **d**, *S.* Typhimurium fecal load of mice as in **c**. Error bar, s.d. Dashed line, detection limit.

the bmK mutants in RAW264.7 macrophages (Fig. 3c), which is less dependent on SPI-1 invasion[43]. These results demonstrate that site-specific lysine butyrylation of HilA modulates *S.* Typhimurium invasion of epithelial cells, consistent with its modulation of HilA-dependent SPI-1 gene expression (Fig. 3a) and secretion of SPI-1 substrates (Fig. 2d).

Since K90 is the most prominent butyrate modification site in HilA (Fig. 1e and Supplementary Table 2), and afforded significantly reduced expression of SPI-1 genes and *S.* Typhimurium infection with bmK incorporation, we focused on this site of HilA modification for additional functional studies. Indeed, HilA butyrylation levels were increased when *S.* Typhimurium was incubated with butyrate (Supplementary Fig. 8b), and K90 site-specific butyrylation was more than doubled (Supplementary Fig. 8c). To investigate site-specific effects of K90 butyrylation, we evaluated HilA occupancy of SPI-1 genes in *S.* Typhimurium. Cross-linking and HA immunoprecipitation–sequencing (x-IP–seq) analysis of HilA-HA *S.* Typhimurium strains showed that HilA-K90bmK-HA had decreased occupancy on the promoter regions of HilA target genes (*prgH* and *invF*) compared to WT HilA-HA (Fig. 4a and Supplementary Fig. 9). Further analysis of HilA-HA variants by cross-linking and HA-immunoprecipitation–qPCR (x-IP–qPCR) revealed site-specific effects of bmK incorporation on HilA-HA DNA binding (Fig. 4b). Indeed, bmK incorporation at K90 and K57 (loss-of-function control) showed markedly less occupancy of *prgH* and *invF* promoters compared to WT HilA and K527 (neutral control) (Fig. 4b). In contrast, bmK incorporation at K324 and K456 had similar HilA-HA occupancy of these SPI-1 locations (Fig. 4b), suggesting that their inhibitory effects may function not through DNA binding, but through alternative mechanisms associated with the predicted TPR domain (Fig. 1c and Supplementary Fig. 10). Interestingly, bmK incorporation at K231 enhanced HilA-HA occupancy at *invF* and *prgH* promoter regions (Fig. 4b), consistent with elevated expression of SPI-1 genes (Fig. 3a) and invasion of HeLa cells (Fig. 3b), suggesting butyrylation of this site may promote HilA oligomerization, DNA binding and/or transcriptional activity. These results demonstrate that site-specific modification of acylated lysine residues directly modulates the function of HilA in *S.* Typhimurium.

Site-specific acylation of HilA affects *Salmonella* dissemination. Given that site-specific bmK incorporation into HilA yielded substantial differences in *S.* Typhimurium infection in vitro, we explored the infectivity of K90 and K231 bmK mutants in vivo. For these studies, we employed the streptomycin-treatment model of *S.* Typhimurium infection in mice[44], which has been shown to deplete butyrate-producing microbiota[16] and provide a SCFA-deficient environment for evaluating site-specific modification of HilA mutants in vivo. Our initial analysis of bmK-labeled HilA-K90-TAG-HA and HilA-K231-TAG-HA *S.* Typhimurium strains showed similar levels of overall pathogenesis on oral infection of streptomycin-treated mice compared to *ΔhilA S.* Typhimurium (Fig. 5a,b), likely due to depletion of bmK and inactivation of full-length HilA protein expression after multiple days in vivo. We thus focused on *S.* Typhimurium dissemination into mesenteric lymph nodes (mLN) and liver early (2 d) postinfection to evaluate acute SPI-1-dependent invasion in vivo. For these experiments, we orally infected streptomycin-treated mice with bmK-labeled WT and HilA mutant *S.* Typhimurium strains, collected their mLN and liver and measured colony-forming units (CFUs) by *Salmonella*-selective agar plates. In comparison to WT *S.* Typhimurium, the bmK-labeled HilA-K90 mutant was defective in dissemination from the intestines, similar

to *ΔhilA*, while the bmK-labeled HilA-K231 mutant was recovered from mLN and liver at similar levels to WT (Fig. 5c). These results are consistent with previous reports of *ΔhilA* in vivo[45], which is more attenuated than mutations in the SPI-1 needle complex alone[46], since HilA also regulates motility and other environmental response elements in *S.* Typhimurium[47]. Moreover, histological analysis of intestinal sections revealed that WT *S.* Typhimurium caused notable inflammation in the mice cecum, whereas the bmK-labeled HilA-K90 mutant had mild to no inflammation in the cecum (Fig. 5d and Supplementary Fig. 11). These results demonstrate that site-specific butyrylation of K90 on HilA nearly phenocopies *ΔhilA* and is sufficient to attenuate *S.* Typhimurium invasion and dissemination in vivo.

Multisite HilA mutant is resistant to butyrate inhibition. Since site-specific HilA lysine butyrylation impaired *S.* Typhimurium virulence, we investigated whether these bacterial strains would be resistant to butyrate inhibition. We initially evaluated K90 to alanine and arginine mutants as potential acylation-deficient mutants, but both single-site mutants showed similar sensitivity to butyrate inhibition of invasion in HeLa cells (Supplementary Fig. 12a). Since K324 and K456 could also be acylated (Supplementary Fig. 3 and Supplementary Table 2) and were inhibited by site-specific bmK incorporation (Fig. 3a,b), we hypothesized that butyrylation of K324 and K456 could still inhibit HilA function and *S.* Typhimurium virulence. We thus tested overexpressed multisite HilA mutants in which K90, K324 and K456 were all mutated to alanine (K90,324,456A) or arginine (K90,324,456R) (Supplementary Fig. 12b). While the HilA-K90,324,456A mutant showed defective SPI-1 secretion activity and was not useful for butyrate inhibition studies (Supplementary Fig. 12b), the HilA-K90,324,456R mutant exhibited similar SPI-1 secretion activity to WT HilA (Supplementary Fig. 12b). We thus generated the HilA-K90,324,456R chromosomal mutant strain, and found that it was resistant to butyrate inhibition of SPI-1 gene expression (Fig. 6a) as well as invasion of HeLa cells (Fig. 6b). We thus explored the infectivity of the HilA-K90,324,456R mutant strain in vivo. Infection of microbiota-sufficient mice containing higher levels of butyrate[16] with the HilA-K90,324,456R mutant strain resulted in shorter survival time compared to WT *S.* Typhimurium (Fig. 6c), which was correlated with a more rapid expansion and shedding of *S.* Typhimurium (Fig. 6d). The difference between WT *S.* Typhimurium and the HilA-K90,324,456R mutant strain was dependent on the microbiota, as streptomycin-treated mice had similar survival time and *S.* Typhimurium fecal load when infected with WT or HilA-K90,324,456R mutant strain (Supplementary Fig. 12c,d). These results further demonstrate that acylation of key virulence factors, such as HilA, by exogenous butyrate may contribute to microbiota attenuation of *S.* Typhimurium infection in vivo.

Discussion

SCFAs are abundant metabolites generated by microbiota fermentation of dietary polysaccharides, but the molecular mechanisms by which these prominent gut metabolites inhibit enteric pathogen virulence have been unclear. For example, propionate generated by Bacteroides is reported to mediate colonization resistance against *S.* Typhimurium and other Enterobacteriaceae by disrupting intracellular pH homeostasis[48,49], as well as destabilizing HilD, another SPI-1 transcriptional regulator[24], suggesting specific mechanisms from different microbiota species and metabolites that may act cooperatively to prevent *S.* Typhimurium infection in vivo. Indeed, our analysis of butyrate associated with other microbiota species revealed that direct acylation of other SPI-1 factors may be another mechanism to attenuate *S.* Typhimurium virulence. The most prominent target from our chemical proteomic studies was HilA, a key transcriptional regulator of SPI-1 genes required for *S.* Typhimurium invasion of intestinal epithelial cells and dissemination in vivo. To functionally evaluate site-specific HilA butyrylation, we installed butyryl-lysine analogs into chromosomally expressed HilA mutants using CRISPR–Cas9 gene editing and noncanonical amino acid mutagenesis. These constitutively butyryl-lysine-modified HilA mutants revealed site-specific effects on *S.* Typhimurium virulence gene expression, invasion of epithelial cells and dissemination in vivo (Supplementary Fig. 13a). Abrogation of acylation on critical lysine residues on HilA results in resistance to butyrate inhibition in vitro and in vivo. While HilA acylation is substoichiometric, it can be increased by the millimolar levels of exogenous butyrate reported in the gut, and may be further regulated by specific microbiota butyrate producers in vivo. *S.* Typhimurium may therefore sense high concentrations of this SCFA through HilA acylation to limit invasion of host cells and utilize butyrate as a nutrient source from the microbiota in the intestinal lumen (Supplementary Fig. 13b). Finally, our finding of inhibitory acylation on specific proteins and amino acid residues suggests repurposing covalent protein modification agents may afford new anti-infectives for SCFA-sensitive pathogens.

Online content

Any methods, additional references, Nature Research reporting summaries, source data, extended data, supplementary information, acknowledgements, peer review information; details of author contributions and competing interests; and statements of data and code availability are available at https://doi.org/10.1038/s41589-019-0392-5.

Received: 4 September 2018; Accepted: 23 September 2019;
Published online: 18 November 2019

References

1. Rooks, M. G. & Garrett, W. S. Gut microbiota, metabolites and host immunity. *Nat. Rev. Immunol.* **16**, 341–352 (2016).
2. Cummings, J. H., Pomare, E. W., Branch, W. J., Naylor, C. P. & Macfarlane, G. T. Short chain fatty acids in human large intestine, portal, hepatic and venous blood. *Gut* **28**, 1221–1227 (1987).
3. Atarashi, K. et al. Induction of colonic regulatory T cells by indigenous *Clostridium* species. *Science* **331**, 337–341 (2011).
4. Donohoe, D. R. et al. The microbiome and butyrate regulate energy metabolism and autophagy in the mammalian colon. *Cell Metab.* **13**, 517–526 (2011).
5. Elinav, E. et al. NLRP6 inflammasome regulates colonic microbial ecology and risk for colitis. *Cell* **145**, 745–757 (2011).
6. Voltolini, C. et al. A novel antiinflammatory role for the short-chain fatty acids in human labor. *Endocrinology* **153**, 395–403 (2012).
7. Trompette, A. et al. Gut microbiota metabolism of dietary fiber influences allergic airway disease and hematopoiesis. *Nat. Med.* **20**, 159–166 (2014).
8. Singh, N. et al. Activation of Gpr109a, receptor for niacin and the commensal metabolite butyrate, suppresses colonic inflammation and carcinogenesis. *Immunity* **40**, 128–139 (2014).
9. Macia, L. et al. Metabolite-sensing receptors GPR43 and GPR109A facilitate dietary fibre-induced gut homeostasis through regulation of the inflammasome. *Nat. Commun.* **6**, 6734 (2015).
10. Furusawa, Y. et al. Commensal microbe-derived butyrate induces the differentiation of colonic regulatory T cells. *Nature* **504**, 446–450 (2013).
11. Arpaia, N. et al. Metabolites produced by commensal bacteria promote peripheral regulatory T-cell generation. *Nature* **504**, 451–455 (2013).
12. Smith, P. M. et al. The microbial metabolites, short-chain fatty acids, regulate colonic T_{reg} cell homeostasis. *Science* **341**, 569–573 (2013).
13. Chang, P. V., Hao, L., Offermanns, S. & Medzhitov, R. The microbial metabolite butyrate regulates intestinal macrophage function via histone deacetylase inhibition. *Proc. Natl Acad. Sci. USA* **111**, 2247–2252 (2014).
14. Schulthess, J. et al. The short chain fatty acid butyrate imprints an antimicrobial program in macrophages. *Immunity* **50**, 432–445.e7 (2019).
15. Byndloss, M. X. et al. Microbiota-activated PPAR-γ signaling inhibits dysbiotic Enterobacteriaceae expansion. *Science* **357**, 570–575 (2017).
16. Rivera-Chávez, F. et al. Depletion of butyrate-producing *Clostridia* from the gut microbiota drives an aerobic luminal expansion of *Salmonella*. *Cell Host Microbe* **19**, 443–454 (2016).
17. Bronner, D. N. et al. Genetic ablation of butyrate utilization attenuates gastrointestinal *Salmonella* disease. *Cell Host Microbe* **23**, 266–273.e4 (2018).

18. Gantois, I. et al. Butyrate specifically down-regulates *Salmonella* pathogenicity island 1 gene expression. *Appl. Environ. Microbiol.* **72**, 946–949 (2006).
19. Lawhon, S. D., Maurer, R., Suyemoto, M. & Altier, C. Intestinal short-chain fatty acids alter *Salmonella typhimurium* invasion gene expression and virulence through BarA/SirA. *Mol. Microbiol.* **46**, 1451–1464 (2002).
20. Groisman, Ea & Ochman, H. Cognate gene clusters govern invasion of host epithelial cells by *Salmonella typhimurium* and *Shigella flexneri*. *EMBO J.* **12**, 3779–3787 (1993).
21. Hentchel, K. L. & Escalante-Semerena, J. C. Acylation of biomolecules in prokaryotes: a widespread strategy for the control of biological function and metabolic stress. *Microbiol. Mol. Biol. Rev.* **79**, 321–346 (2015).
22. Yang, Y.-Y., Ascano, J. M. & Hang, H. C. Bioorthogonal chemical reporters for monitoring protein acetylation. *J. Am. Chem. Soc.* **132**, 3640–3641 (2010).
23. Grammel, M. & Hang, H. C. Chemical reporters for biological discovery. *Nat. Chem. Biol.* **9**, 475–484 (2013).
24. Hung, C.-C. C. et al. The intestinal fatty acid propionate inhibits *Salmonella* invasion through the post-translational control of HilD. *Mol. Microbiol.* **87**, 1045–1060 (2013).
25. Sang, Y. et al. Acetylation regulating protein stability and DNA-binding ability of HilD, thus modulating *Salmonella* Typhimurium virulence. *J. Infect. Dis.* **216**, 1018–1026 (2017).
26. Lostroh, C. P., Bajaj, V. & Lee, C. A. The *cis* requirements for transcriptional activation by HilA, a virulence determinant encoded on SPI-1. *Mol. Microbiol.* **37**, 300–315 (2000).
27. Bajaj, V., Lucas, R. L., Hwang, C. & Lee, C. A. Co-ordinate regulation of *Salmonella typhimurium* invasion genes by environmental and regulatory factors is mediated by control of hilA expression. *Mol. Microbiol.* **22**, 703–714 (1996).
28. Ellermeier, J. R. & Slauch, J. M. Adaptation to the host environment: regulation of the SPI1 type III secretion system in *Salmonella enterica* serovar Typhimurium. *Curr. Opin. Microbiol.* **10**, 24–29 (2007).
29. Bajaj, V., Hwang, C. & Lee, C. A. hilA is a novel ompR/toxR family member that activates the expression of *Salmonella typhimurium* invasion genes. *Mol. Microbiol.* **18**, 715–727 (1995).
30. Lostroh, C. P. & Lee, C. A. The HilA box and sequences outside it determine the magnitude of HilA-dependent activation of P_{prgH} from *Salmonella* pathogenicity island 1. *J. Bacteriol.* **183**, 4876–4885 (2001).
31. Eichelberg, K. & Galan, J. E. Differential regulation of *Salmonella typhimurium* type III secreted proteins by pathogenicity island 1 (SPI-1)-encoded transcriptional activators InvF and HilA. *Infect. Immun.* **67**, 4099–4105 (1999).
32. Boddicker, J. D., Knosp, B. M. & Jones, B. D. Transcription of the *Salmonella* invasion gene activator, hilA, requires HilD activation in the absence of negative regulators. *J. Bacteriol.* **185**, 525–533 (2003).
33. Christensen, D. G. et al. Identification of novel protein lysine acetyltransferases in *Escherichia coli*. *MBio* **9**, e01905–e01918 (2018).
34. Sturm, A. *Bistable Regulation of ttss-1 Genes in* Salmonella *Typhimurium*. Doctoral Thesis, ETH Zürich (2011); https://doi.org/10.3929/ethz-a-006715280
35. Kim, D. E., Chivian, D. & Baker, D. Protein structure prediction and analysis using the Robetta server. *Nucleic Acids Res.* **32**, W526–W531 (2004).
36. Chin, J. W. Expanding and reprogramming the genetic code. *Nature* **550**, 53–60 (2017).
37. Gattner, M. J., Vrabel, M. & Carell, T. Synthesis of ε-*N*-propionyl-, ε-*N*-butyryl-, and ε-*N*-crotonyl-lysine containing histone H3 using the pyrrolysine system. *Chem. Commun.* **49**, 379–381 (2013).
38. Neumann, H., Peak-Chew, S. Y. & Chin, J. W. Genetically encoding N^{ε}-acetyllysine in recombinant proteins. *Nat. Chem. Biol.* **4**, 232–234 (2008).
39. Li, J. et al. Ligand-free palladium-mediated site-specific protein labeling inside gram-negative bacterial pathogens. *J. Am. Chem. Soc.* **135**, 7330–7338 (2013).
40. Zhang, M. et al. A genetically incorporated crosslinker reveals chaperone cooperation in acid resistance. *Nat. Chem. Biol.* **7**, 671–677 (2011).
41. Lin, S. et al. Site-specific incorporation of photo-cross-linker and bioorthogonal amino acids into enteric bacterial pathogens. *J. Am. Chem. Soc.* **133**, 20581–20587 (2011).
42. Jiang, W., Bikard, D., Cox, D., Zhang, F. & Marraffini, La RNA-guided editing of bacterial genomes using CRISPR–Cas systems. *Nat. Biotechnol.* **31**, 233–239 (2013).
43. Drecktrah, D., Knodler, L. A., Ireland, R. & Steele-Mortimer, O. The mechanism of *Salmonella* entry determines the vacuolar environment and intracellular gene expression. *Traffic* **7**, 39–51 (2006).
44. Barthel, M. et al. Pretreatment of mice with streptomycin provides a *Salmonella enterica* serovar Typhimurium colitis model that allows analysis of both pathogen and host. *Infect. Immun.* **71**, 2839–2858 (2003).
45. Ellermeier, C. D., Ellermeier, J. R. & Slauch, J. M. HilD, HilC and RtsA constitute a feed forward loop that controls expression of the SPI1 type three secretion system regulator hilA in *Salmonella enterica* serovar Typhimurium. *Mol. Microbiol.* **57**, 691–705 (2005).
46. Hapfelmeier, S. et al. The *Salmonella* pathogenicity island (SPI)-2 and SPI-1 type III secretion systems allow *Salmonella* serovar Typhimurium to trigger colitis via MyD88-dependent and MyD88-independent mechanisms. *J. Immunol.* **174**, 1675–1685 (2005).
47. Thijs, I. M. V. et al. Delineation of the *Salmonella enterica* serovar Typhimurium HilA regulon through genome-wide location and transcript analysis. *J. Bacteriol.* **189**, 4587–4596 (2007).
48. Jacobson, A. et al. A gut commensal-produced metabolite mediates colonization resistance to *Salmonella* infection. *Cell Host Microbe* **24**, 296–307.e7 (2018).
49. Sorbara, M. T. et al. Inhibiting antibiotic-resistant Enterobacteriaceae by microbiota-mediated intracellular acidification. *J. Exp. Med.* **216**, 84–98 (2019).
50. Santiviago, C. A. et al. Analysis of pools of targeted *Salmonella* deletion mutants identifies novel genes affecting fitness during competitive infection in mice. *PLoS Pathog.* **5**, e1000477 (2009).

Publisher's note Springer Nature remains neutral with regard to jurisdictional claims in published maps and institutional affiliations.

© The Author(s), under exclusive licence to Springer Nature America, Inc. 2019

Methods

Microbial strains and growth conditions. All strains used are listed in Supplementary Table 4. All *S.* Typhimurium strains used were derivatives of *S.* Typhimurium 14028S (ref. [24]). The *S.* Typhimurium *ΔhilA* mutant was from *Salmonella enterica* subsp. *enterica*, Strain 14028S (Serovar Typhimurium) single-gene deletion mutant library[50]. *Salmonella* strains were cultured at 37 °C in liquid LB medium (10 g l^{-1} tryptone, 5 g l^{-1} yeast extract, 10 g l^{-1} NaCl) (Becton Dickinson, Difco), SPI-1-inducing LB medium (10 g l^{-1} tryptone, 5 g l^{-1} yeast extract, 300 mM NaCl) or on *Salmonella–Shigella* agar (Becton Dickinson). Cultures were grown at 37 °C in Multitron shaking incubator (INFORS HT) at 220 r.p.m. When required, antibiotics were added to the medium as follows: carbenicillin 100 μg ml^{-1}, kanamycin 50 μg ml^{-1} and chloramphenicol 10 μg ml^{-1}.

Animal experiments. C57BL/6J (catalog no. 000664) mice were purchased from the Jackson Laboratory and maintained at the Rockefeller University animal facilities under specific-pathogen-free conditions. Animal care and experimentation were consistent with the National Institutes of Health (NIH) guidelines and approved by the Institutional Animal Care and Use Committee of the Rockefeller University.

Chemicals. Sodium butyrate was purchased from Sigma-Aldrich (catalog no. 303410). Alk-3 (4-pentynoic acid) was purchased from Sigma-Aldrich (catalog no. 232211). Azide-rhodamine was synthesized in the laboratory as previously described[51]. Azide-biotin was purchased from Sigma-Aldrich (catalog no. 762024). Butyryl-lysine was synthesized as previously described[37]. BmK was synthesized as previously described[39].

Generation of HilA-K90bu site-specific antibody. HilA-K90bu peptide (CRILSED(butyrylK)EHRYIE) and HilA-K90 peptide (CRILSEDKEHRYIE) were synthesized in The Rockefeller University Proteomics Resource Center. HilA-K90bu peptide was sent to Thermo Fisher for custom antibody production with a 70-day rabbit immunization protocol. Serum was collected on days 35, 56 and 58 and measured for titer with ELISA. Site-specific polyclonal antibodies were affinity purified and counter-selected with HilA-K90 peptide.

***Salmonella* growth curve.** Overnight cultures of *Salmonella* strains in LB medium were diluted 1:100 to 5 ml fresh SPI-1-inducing LB medium in Falcon round-bottomed 15-ml tubes. Cultures were taken out as aliquots of 750 μl from 0 h to 5 h at 1-h intervals. Aliquots were added to 10 mm polystyrene cuvettes (Sarstedt) and the optical density (OD_{600}) was measured with a Biophotometer plus (Eppendorf).

Preparation of *Salmonella* bacterial total cell lysates. Dilutions (1:50) of overnight LB medium cultures of *S.* Typhimurium strain 14028S WT were grown in 4 ml SPI-1-inducing LB medium for 4 h at 37 °C with 220 r.p.m. shaking. For alk-3-labeling experiments, cultures were incubated with or without 10 mM fresh alk-3 (in dH_2O). For incorporation of noncoding amino acids into overexpressed HilA, cultures were added with 1 mM noncanonical amino acids and 0.2% arabinose. For incorporation of noncoding amino acids into endogenous HilA, cultures were added with 100 μM noncoding amino acids and 0.01% arabinose. *S.* Typhimurium cells were pelleted at 15,000*g* for 1 min, and pellets were lysed with 200 μl lysis buffer (PBS containing 0.5% Nonidet P-40, 1× EDTA-free protease inhibitor cocktail (Roche), 0.5 mg ml^{-1} lysozyme (in dH_2O) (Sigma) and 1:1,000 dilution of Benzonase (Millipore)). After resuspension, pellets were sonicated for 10 s, three times, then incubated on ice for 30 min. Cell lysates were centrifuged at 15,000*g* for 1 min to remove cell debris and supernatants were collected. Protein concentration was estimated by BCA assay with the BCA Protein Assay Kit (Thermo Fisher).

***Salmonella* protein immunoprecipitation and immunoblotting.** From *Salmonella* total cell lysates prepared as described above, protein samples were boiled with 1× Laemmli buffer 95 °C for 5 min. For each sample, 20 μl was loaded onto a 4–20% Tris–HCl gel (Bio-Rad) for SDS–PAGE. Proteins were transferred onto 0.45-μm nitrocellulose membrane (Bio-Rad) with Trans-Blot Turbo Transfer System (Bio-Rad) at 25 V for 30 min. Membrane was blocked with 5% nonfat milk in PBS with 0.1% Tween-20 (PBS-T) for 30 min, and primary antibody was added to the solution before incubating membrane at 4 °C overnight. Dilution of primary antibodies was as follows: for HA-tagged proteins, 1:2,000 anti-HA rabbit antibody (Sigma-Aldrich, catalog no. H6908); for FLAG-tagged proteins, 1:2,000 anti-FLAG rabbit antibody (Sigma-Aldrich, catalog no. F7425); for HilA-K90Bu antigen, 1:200 anti-HilA-K90Bu rabbit custom antibody (Thermo Fisher) or 1:200 anti-HilA K90 rabbit custom antibody (Thermo Fisher). Membrane was washed three times with PBS-T and incubated with 1:10,000 goat polyclonal anti-rabbit HRP (Abcam, catalog no. ab97051) in PBS-T with 5% nonfat milk at room temperature for 1 h. Membrane was washed three times with PBS-T, and imaged with Clarity Western ECL substrate (Bio-Rad) and the ChemiDoc XRS+ System (Bio-Rad).

For *Salmonella* protein immunoprecipitation, 250 μg of each total cell lysate was incubated with 20 μl PBS-T-washed EZview Red Anti-HA Affinity Gel (Sigma-Aldrich) at 4 °C for 1 h with end-to-end rotation. Samples were washed three times with 200 μl PBS-T before being boiled with 1× Laemmli buffer at 95 °C for 5 min. Each sample (20 μl) was loaded onto a 4–20% Tris–HCl gel (Bio-Rad) for SDS–PAGE and further immunoblotting.

In-gel fluorescence analysis of alk-3 labeling. For in-gel fluorescence analysis of alk-3-labeled *Salmonella* proteome, from the alk-3-treated or control total cell lysates prepared as described above, 45 μl of each total cell lysate (~50 μg) was added with 5 μl of click chemistry reagents as a 10× master mix (az-Rho: 0.1 mM, 10 mM stock solution in DMSO; tris(2-carboxyethyl)phosphine hydrochloride (TCEP): 1 mM, 50 mM freshly prepared stock solution in dH_2O; tris[(1-benzyl -1*H*-1,2,3-triazol-4-yl)methyl]amine (TBTA): 0.1 mM, 2 mM stock in 4:1 *t*-butanol:DMSO; $CuSO_4$: 1 mM, 50 mM freshly prepared stock in dH_2O. Samples were mixed well and incubated at room temperature for 1 h. After incubation, samples were mixed with 200 μl cold methanol, 150 μl cold water and 75 μl cold chloroform. Sample proteins were precipitated at 18,000*g* for 1 min at 4 °C. After gently removing the aqueous layer, protein pellets were washed with 200 μl cold methanol, spinning down at 18,000*g* for 1 min at 4 °C and liquid was gently decanted. After washing twice, pellets were air-dried before boiling with 1× Laemmli buffer.

For in-gel fluorescence analysis of alk-3-labeled HilA, from the alk-3-treated or control total-cell lysates prepared as described above, 250 μg of each total cell lysate was immunoprecipitated with 20 μl PBS-T-washed EZview Red Anti-HA Affinity Gel (Sigma-Aldrich). After samples were washed three times with 200 μl PBS-T, 36 μl of PBS was added to each sample and 4 μl of click chemistry reagents as a 10× master mix, as described above, were added to each sample. Samples were mixed well and incubated at room temperature for 1 h. After incubation, samples were washed three times with 200 μl PBS-T.

Samples were boiled with 1× Laemmli buffer 95 °C for 5 min before being loaded onto a 4–20% Tris–HCl gel (Bio-Rad) for SDS–PAGE. In-gel fluorescence scanning was performed using a Typhoon 9400 imager (Amersham Biosciences).

Alk-3-labeling LQF proteomics. Dilutions (1:50) of overnight LB cultures of *S.* Typhimurium strain 14028s WT were grown in 20 ml SPI-1-inducing LB medium for 4 h at 37 °C with 220 r.p.m. shaking, with each sample growing in 4-ml aliquots. Cultures were incubated with or without 10 mM fresh alk-3 (in dH_2O). Cultures were pooled back to 20 ml per sample in Falcon tubes and lysed in lysis buffer as described above. After resuspension in 1 ml lysis buffer, bacteria were sonicated for 15 s with a Sonic Dismembrator Model 500 (Fisher Scientific) with 5 s on and 10 s off per cycle. Cell lysates were centrifuged at 15,000*g* for 1 min to remove cell debris, and supernatants were collected. Each total cell lysate (~2 mg) was added with 100 μl of click chemistry reagents as a 10× master mix (az-biotin: 0.1 mM, 10 mM stock solution in DMSO; TCEP: 1 mM, 50 mM freshly prepared stock solution in dH_2O; TBTA: 0.1 mM, 2 mM stock in 4:1 *t*-butanol:DMSO; $CuSO_4$: 1 mM, 50 mM freshly prepared stock in dH_2O. Samples were mixed well and incubated at room temperature for 1 h. After incubation, samples were mixed with 4 ml cold methanol and incubated at −20 °C overnight. Protein pellets were centrifuged at 5,000*g* for 30 min at 4 °C, and were washed three times with 1 ml cold methanol. After the last wash, pellets were air-dried before being re-solubilized in 250 μl 4% SDS–PBS with bath sonication. Solutions were diluted with 750 μl PBS and incubated with 60 μl PBS-T-washed High Capacity NeutrAvidin agarose (Pierce) at room temperature for 1 h with end-to-end rotation. Agarose was washed three times with 500 μl 1% SDS–PBS, three times with 500 μl 2 M urea–PBS and three times with 500 μl PBS. Agarose was then reduced with 100 μl 10 mM DTT (Sigma-Aldrich) in PBS for 30 min at 37 °C, and alkylated with 100 μl 50 mM iodoacetamide (Sigma-Aldrich) in PBS for 20 min in the dark. On-bead proteins were digested with 400 ng Trypsin/Lys-C mix (Promega) at 37 °C overnight, with shaking. Digested peptides were collected and lyophilized before being desalted with a custom-made stage-tip containing Empore SPE Extraction Disk (3M). Peptides were eluted with 2% acetonitrile and 2% formic acid in dH_2O.

Peptide LC–MS analysis was performed as described previously[52]. Briefly, samples were analyzed with a Dionex 3000 nano-HPLC coupled to an Orbitrap XL mass spectrometer (Thermo Fisher). Peptide samples were pressure-loaded onto a homemade C18 reverse-phase column (75 μm diameter, 15 cm length). A 180-min gradient from 95% buffer A (HPLC grade water with 0.1% formic acid) and 5% buffer B (HPLC grade acetonitrile with 0.1% formic acid) to 25% buffer A and 75% buffer B in 133 min was used at 200 nl min^{-1}. The Orbitrap XL was operated in top-8-CID mode with MS spectra measured at a resolution of 60,000 at m/z 400. One full MS scan (300–2000 MW) was followed by three data-dependent scans of the *n*th most intense ions with dynamic exclusion enabled. Peptides fulfilling a Percolator-calculated 1% false discovery rate threshold were reported.

LQF of alk-3-labeled proteins was performed with the label-free MaxLFQ algorithm in MaxQuant software, as described[53]. The search results from MaxQuant were analyzed by Perseus (http://www.perseusframework.org/). Briefly, the control replicates and alk-3-labeled sample replicates were grouped correspondingly. The results were cleaned to filter off reverse hits and contaminants. Only proteins that were identified in all alk-3-labeled sample replicates, and with more than two unique peptides, were subjected to subsequent statistical analysis. LFQ intensities were used for measuring protein abundance and were logarithmized. Signals that were originally zero were imputed with random numbers from a normal distribution, whose mean and standard deviation

were chosen to best simulate low abundance values below the noise level (Replace missing values by normal distribution with Width = 0.3 and Shift = 2.2). Significant proteins enriched in the alk-3-labeled sample group versus control group were determined by a threshold strategy, in which a ratio larger than or equal to 2 and a *P* value smaller than 0.05 were categorized as hits. The resulting table was exported as Supplementary Dataset 1.

MS/MS detection of protein post-translational modifications. Dilutions (1:50) of overnight LB cultures of *S.* Typhimurium strain 14028s Δ*hilA* pBAD-HilA-HA-His overnight culture were grown in 500 ml SPI-1-inducing LB medium with 10 mM sodium propionate or 10 mM sodium butyrate for 2 h at 37 °C with 220 r.p.m. shaking, before 0.2% arabinose was added to induce HilA-HA-His expression for 3 h. Bacteria were collected with 5,000*g* for 10 min at 4 °C and lysed in 25 ml lysis buffer as described above with 1 mM EDTA and 50 mM nicotinamide (NAM). Bacteria were sonicated for 5 min with a Sonic Dismembrator Model 500 (Fisher Scientific) with 5 s on and 10 s off per cycle. Lysates were centrifuged at 5,000*g* for 10 min at 4 °C, and supernatants were filtered with a 0.22 μm filter, before being loaded onto a HisTrap FF 5 ml column (GE Healthcare). HilA-HA-His protein was purified with washing with three column volume (CV) 100% buffer A (PBS-T, 50 mM NAM), washing with 5 CV 10% buffer B (PBS-T, 50 mM NAM, 300 mM imidazole) and 5 CV elution with gradient from 10% to 100% buffer B. Fractions containing HilA were pooled and dialyzed to PBS-T with three spin–dilution cycles in 10,000 MWCO filter (Amicon). Purified HilA-HA-His was immunoprecipitated with anti-butyryl-lysine antibody- (PTM Biolab) or anti-propionyl-lysine antibody (PTM Biolab)-conjugated protein A/G magnetic beads (Pierce), and samples were boiled and run on SDS–PAGE. Coomassie Blue-stained bands corresponding to HilA were cut out, reduced with 10 mM DTT (Sigma-Aldrich) in fresh 100 mM ammonium bicarbonate for 30 min at 37 °C, and alkylated with 50 mM iodoacetamide (Sigma-Aldrich) in fresh 100 mM ammonium bicarbonate for 20 min in the dark. Gel pieces were digested with 200 ng Trypsin/Lys-C mix (Promega) at 37 °C overnight, with shaking.

***Salmonella* CRISPR–Cas9 genome editing.** To make electrocompetent *S.* Typhimurium, overnight culture of *S.* Typhimurium strains were diluted 1:50 to 100 ml fresh LB medium, and were grown at 37 °C in a shaking incubator at 220 r.p.m. for 2 h, until the OD_{600} reached 0.5–0.7. Cells were pelleted at 5,000*g* for 10 min at 4 °C, and washed twice with 50 ml ice-cold 10% glycerol. Cell pellets were resuspended in 500 μl 10% glycerol, and aliquoted as 50 μl per tube. Electrocompetent parent *S.* Typhimurium strains were transformed with pKD46 via electroporation with Gene Pulser II (Bio-Rad) at 2.5 kV and 25 μF in a 2-mm cuvette, and selected on ampicillin agar plates at 30 °C overnight. The resulting *S.* Typhimurium pKD46 strains were made into electrocompetent cells after being grown at 30 °C with 0.2% arabinose and ampicillin. *S.* Typhimurium pKD46 electrocompetent cells were transformed with 2 μl pWJ297-sgRNA (single guide RNA) (~100 ng) and 10 μl 10 μM ssDNA editing template and selected on chloramphenicol agar plates at 37 °C overnight. All colonies on the plate were collected with a cell scraper and resuspended in 4 ml LB medium with chloramphenicol. The bacterial suspensions were diluted 1:50 to 4 ml fresh LB medium with chloramphenicol, and were grown at 37 °C in a Multitron shaking incubator (INFORS HT) at 220 r.p.m. for 2 h. Culture was streaked onto chloramphenicol agar plates, and colonies from the plates were randomly picked for colony PCR to confirm successful editing. Successfully edited colonies were streaked onto plain agar plates to cure pWJ297-sgRNA, and curing was confirmed by streaking on chloramphenicol agar plates.

Optimization of *Salmonella* CRISPR–Cas9 genome editing was performed as follows. The protocol for CRISPR–Cas9 genome editing in *E. coli*[42] resulted in a very high false-positive rate and an estimated editing efficiency of less than 5% (data not shown). To increase editing efficiency, we introduced synonymous co-mutation of the nearest protospacer adjacent motif (PAM), together with targeted sequence, and used guide RNA specific for that PAM to guide Cas9 (Supplementary Fig. 5a). As an example, we set out to mutate Lys 90 to Ala in HilA. Synonymous PAM co-mutation (C243G) increased editing efficiency and resulted in successful editing (Supplementary Fig. 5b). Colonies selected for pWJ297 (pCas9) and pCRISPR were mostly false-positive, meaning that the CRISPR–Cas9 system did not impose an adequate selection pressure. We surmised that *Salmonella* has an intrinsic suppressive mechanism to inactivate the exogenous CRISPR–Cas9 system. Therefore, we collected all colonies from the plate of first-round selection, suspended them in liquid LB medium with corresponding antibiotics and grew them to early stationary phase. The resulting culture was plated again on selection agar plates. This liquid selection protocol drastically increased the frequency of successfully edited clones (Supplementary Fig. 5c). The plasmid pCRISPR is very resistant to curing, taking up to one month of serial purification (data not shown), which is presumably due to its small size and high copy number. Therefore, we incorporated sgRNA sequence directly at the pWJ297 BsaI cloning site, sparing the usage of pCRISPR. The editing efficiency of pWJ297-sgRNA is similar to that of the pWJ297 + pCRISPR combination (data not shown), while the former was cured in about 1 d. Single-stranded DNA recombination efficiency is much higher than double-stranded DNA (dsDNA) in *E. coli* because ssDNA has a higher transformation efficiency[54]. Therefore, we decided to use an ssDNA template when editing site-specific mutation of single codons. CRISPR–Cas9 genome editing with ssDNA provided higher editing efficiency compared to that with a long dsDNA template that has the same mutation site (Supplementary Fig. 5d). We observed no significant difference of editing efficiency among ssDNA templates that matched either the same strand or the complementary strand of the sgRNA, nor between templates matching either the leading or the lagging strand of the genome (Supplementary Fig. 5e). To summarize, we have optimized the scarless CRISPR–Cas9 genome-editing protocol to facilitate the editing process in *Salmonella*, which only takes 3–4 days (Supplementary Fig. 6).

***Salmonella* whole-genome sequencing.** *Salmonella* cultures (1 ml) were processed with Quick-DNA Fungal/Bacterial kit (Zymo Research) according to the manufacturer's manual. Purified *Salmonella* genomes were sent to Rockefeller University Genomics Center for processing with Nextera XT gDNA library preparation and sequencing with MiSeq 75 pair-end sequencing. Sequencing results were analyzed with Geneious software.

***Salmonella* qRT–PCR.** *Salmonella* cultures (500 μl) were processed with RNeasy Mini Kit (Qiagen) according to the manufacturer's manual. Concentrations of purified RNA were normalized to 100 ng μl^{-1} with RNase-free water. qRT–PCR was performed with a Power SYBR Green RNA-to-C_T 1-Step Kit (Applied Biosystems) according to the manufacturer's manual and primers are listed in Supplementary Table 5.

***Salmonella* HilA cross-link IP–qPCR and cross-link IP–seq.** *Salmonella* cultures (4 ml) were cross-linked with 1% methanol-free paraformaldehyde (Thermo Fisher) for 20 min at room temperature. Cross-linking was quenched with 125 mM glycine (Thermo Fisher). Bacteria were centrifuged at 16,000*g* at 4 °C for 1 min and washed twice with 1 ml PBS. Pellets were resuspended in 500 μl ChIP Lysis Buffer (10 mM Tris–HCl, pH 8.0, 20% sucrose, 50 mM NaCl, 10 mM EDTA, 10 mg ml^{-1} lysozyme) and incubated at 37 °C for 30 min. Lysates were added with 500 μl 2× RIPA buffer (100 mM Tris–HCl, pH 8.0, 300 mM NaCl, 2% Nonidet P-40 (NP-40), 1% sodium deoxycholate, 0.2% SDS) and sonicated with a Sonic Dismembrator Model 500 (Fisher Scientific) for 10 s. The resulting solutions were centrifuged at 16,000*g* for 1 min at room temperature. Supernatants (100 μl) were saved as total inputs. For the remaining supernatants, 750 μl of each was incubated with 2 μl anti-HA ChIP-grade polyclonal antibody (Abcam, catalog no. ab9110) at 4 °C for 1 h with end-to-end rotation. The solutions were then added to 30 μl PBS-T-washed protein A/G magnetic beads (Pierce) and incubated at 4 °C for 1 h with end-to-end rotation. Beads were washed twice with 500 μl 1× RIPA buffer, twice with 500 μl LiCl wash buffer (10 mM Tris–HCl, pH 8.0, 250 mM LiCl, 1 mM EDTA, 0.5% NP-40, 0.5% sodium deoxycholate) and once with 500 μl Tris–EDTA buffer (10 mM Tris–HCl, pH 8.0, 1 mM EDTA). Samples were eluted with 100 μl SDS elution buffer (50 mM Tris–HCl, pH 8.0, 10 mM EDTA, 1% SDS) at 65 °C for 10 min. Each total input sample and ChIP sample were added with 5 μl 20 mg ml^{-1} proteinase K (Qiagen) and de-cross-linked at 65 °C overnight. All de-cross-linked samples were purified with E.Z.N.A. Cycle Pure kit (Omega Bio-tek) and eluted with 100 μl elution buffer in the kit. ChIP–qPCR was performed with PowerUp SYBR Green Master Mix (Applied Biosystems) according to the manufacturer's manual and primers are listed in Supplementary Table 5. The same samples were sent to Rockefeller University Genomics Center for library preparation and sequenced with NextSeq High Output 75 Single-Read sequencing.

In vitro invasion assay and intracellular survival assay. HeLa cells were cultured in 12-well tissue culture plates at 80–90% confluency. Wells were added with *Salmonella* cells at a muliplicity of infection (MOI) = 10:1 and centrifuged at 1,000*g* for 5 min. Cells were incubated at 37 °C with 5% CO_2 for 30 min to allow invasion. The media was then replaced with medium containing 100 μg ml^{-1} gentamicin and incubated for an additional hour to kill extracellular *Salmonella*. Wells were then washed three times with PBS, and cells were lysed with 500 μl 1% Triton X-100 PBS. Lysates were serially diluted and drip-dropped on *Salmonella–Shigella* agar plates (Becton Dickinson, catalog no. 211597) to determine the number of invaded bacteria.

For the intracellular survival assay of *Salmonella*, after incubation with medium containing 100 μg ml^{-1} gentamicin for 1 h, media was replaced with medium containing 10 μg ml^{-1} gentamicin and incubated for an additional 4.5 h at 37 °C, 5% CO_2. Intracellular bacterial counts were obtained by lysing cells and drip-dropping serial dilutions on *Salmonella–Shigella* agar plates.

***S.* Typhimurium infection of mice.** For streptomycin-treatment experiments, C57BL/6J specific-pathogen-free mice were gavaged with a single dose of 20 mg of streptomycin 24 h before infection. Bacterial cultures of different *S.* Typhimurium strains were washed and resuspended in sterile PBS at 10^7 CFU ml^{-1}. Mice were gavaged with 100 μl of the bacterial suspension (10^6 CFU). Leftover inocula were serially diluted and plated to confirm the number of CFU administered.

For 48-h infection experiments, mice were euthanized 48 h after *S.* Typhimurium gavage. CFU in the livers and mesenteric lymph nodes (mLN) were determined by plating five serial dilutions of livers or mLN suspended in sterile 0.1% Triton X-100 PBS on *Salmonella–Shigella* agar (Becton Dickinson, catalog no. 211597). Resulting quantities were normalized to liver or mLN weight.

For the *S.* Typhimurium infection survival assay, weight loss of mice was monitored starting just before infection, and mice were euthanized when they reached 80% baseline weight, appeared hunched or moribund or exhibited a visibly distended abdomen (indicative of peritoneal effusion), whichever occurred first. Death was not used as an end-point.

Quantification and statistical analysis. Comparisons and statistical tests were performed as indicated in each figure legend. Briefly, pairwise comparisons were generated with two-tailed *t*-tests. For comparisons of multiple groups over time, or with two variables, a two-way analysis of variance (ANOVA) was used with an appropriate Bonferroni post-test comparing all groups to each other, all groups to a control or selected groups to each other. Survival data were analyzed using a log-rank (Mantel–Cox) test with a Bonferroni correction for the degrees of freedom based on the number of comparisons made. To compare two groups with nonnormal distribution or low sample size, the medians of the two groups were compared using a Mann–Whitney *U*-test, unless one dataset contained only zero values. In these cases, a Mann–Whitney *U*-test could not be performed because all values in the group were identical; a Wilcoxon test was performed instead. For comparisons of multiple groups with only one variable, a one-way ANOVA or Kruskal–Wallis test was performed for data with underlying normal or nonnormal distribution, respectively, with Bonferroni, Dunnett's or Dunn's post-tests where appropriate. Statistical analyses were performed in GraphPad Prism software. A P value of less than 0.05 was considered significant, denoted as $^{*}P \leq 0.05$, $^{**}P \leq 0.01$ and $^{***}P \leq 0.001$ for all analyses.

Reporting Summary. Further information on research design is available in the Nature Research Reporting Summary linked to this article.

Data availability

The data and materials that support the findings of this study are available from the corresponding author upon reasonable request.

References

51. Rangan, K. J., Yang, Y.-Y., Charron, G. & Hang, H. C. Rapid visualization and large-scale profiling of bacterial lipoproteins with chemical reporters. *J. Am. Chem. Soc.* **132**, 10628–10629 (2010).
52. Peng, T. & Hang, H. C. Bifunctional fatty acid chemical reporter for analyzing S-palmitoylated membrane protein–protein interactions in mammalian cells. *J. Am. Chem. Soc.* **137**, 556–559 (2015).
53. Cox, J. et al. Accurate proteome-wide label-free quantification by delayed normalization and maximal peptide ratio extraction, termed MaxLFQ. *Mol. Cell. Proteom.* **13**, 2513–2526 (2014).
54. Court, D. L., Sawitzke, Ja & Thomason, L. C. Genetic engineering using homologous recombination. *Annu. Rev. Genet.* **36**, 361–388 (2002).

Acknowledgements

We thank M. T. Mark, H. Zebroski and H. Molina at The Rockefeller Proteomics Resource Center for LC–MS analyses and butyrylated peptide synthesis. We thank Weill Cornell School of Medicine Electron Microscopy and Histology Core and Memorial Sloan-Kettering Cancer Center Pathology Core for assistance with histology sample preparation and scoring. We thank S. Lin and P. Chen (Peking University) for *Salmonella* amber codon expression plasmids, W. Jiang and L. Marraffini (Rockefeller University) for bacterial CRISPR–Cas9 plasmids, H. Andrews-Polymenis (Texas A&M College of Medicine) and M. McClelland (University of California, Irvine) for *S.* Typhimurium Δ*hilA* strain from NIAID, NIH: *Salmonella enterica* subsp. *enterica*, strain 14028S (serovar Typhimurium) single-gene deletion mutant library, J. Slauch (University of Illinois at Urbana-Champaign) for *S.* Typhimurium *tetRA-hilD-3xFlag* strain, C.-C. Hung and C. Altier (Cornell University) for providing *S.* Typhimurium strain 14028S and helpful discussions and J. Galan (Yale University) for helpful discussions. Z.J.Z. received support from the David Rockefeller Graduate Program. H.C.H. acknowledges support from NIH grants (R01GM087544 and R01AT007671) and the Lerner Trust.

Author contributions

H.C.H. conceived the project, Z.J.Z. and V.A.P. performed experiments and data analysis, T.P. synthesized bmK, Z.J.Z. and H.C.H. wrote the paper, and all authors contributed to manuscript editing.

Competing interests

The authors declare no competing interests.

Additional information

Supplementary information is available for this paper at https://doi.org/10.1038/s41589-019-0392-5.

Correspondence and requests for materials should be addressed to H.C.H.

Reprints and permissions information is available at www.nature.com/reprints.

nature research

Corresponding author(s): Howard C. Hang

Reporting Summary

Nature Research wishes to improve the reproducibility of the work that we publish. This form provides structure for consistency and transparency in reporting. For further information on Nature Research policies, see Authors & Referees and the Editorial Policy Checklist.

Statistical parameters

When statistical analyses are reported, confirm that the following items are present in the relevant location (e.g. figure legend, table legend, main text, or Methods section).

n/a	Confirmed	
☐	☒	The exact sample size (*n*) for each experimental group/condition, given as a discrete number and unit of measurement
☐	☒	An indication of whether measurements were taken from distinct samples or whether the same sample was measured repeatedly
☐	☒	The statistical test(s) used AND whether they are one- or two-sided *Only common tests should be described solely by name; describe more complex techniques in the Methods section.*
☒	☐	A description of all covariates tested
☐	☒	A description of any assumptions or corrections, such as tests of normality and adjustment for multiple comparisons
☐	☒	A full description of the statistics including central tendency (e.g. means) or other basic estimates (e.g. regression coefficient) AND variation (e.g. standard deviation) or associated estimates of uncertainty (e.g. confidence intervals)
☐	☒	For null hypothesis testing, the test statistic (e.g. *F*, *t*, *r*) with confidence intervals, effect sizes, degrees of freedom and *P* value noted *Give P values as exact values whenever suitable.*
☒	☐	For Bayesian analysis, information on the choice of priors and Markov chain Monte Carlo settings
☒	☐	For hierarchical and complex designs, identification of the appropriate level for tests and full reporting of outcomes
☒	☐	Estimates of effect sizes (e.g. Cohen's *d*, Pearson's *r*), indicating how they were calculated
☐	☒	Clearly defined error bars *State explicitly what error bars represent (e.g. SD, SE, CI)*

Our web collection on statistics for biologists may be useful.

Software and code

Policy information about availability of computer code

Data collection	No software was used.
Data analysis	GraphPad Prism 5.0, Geneious 11.0

For manuscripts utilizing custom algorithms or software that are central to the research but not yet described in published literature, software must be made available to editors/reviewers upon request. We strongly encourage code deposition in a community repository (e.g. GitHub). See the Nature Research guidelines for submitting code & software for further information.

Data

Policy information about availability of data

All manuscripts must include a data availability statement. This statement should provide the following information, where applicable:

- Accession codes, unique identifiers, or web links for publicly available datasets
- A list of figures that have associated raw data
- A description of any restrictions on data availability

The data that support the findings of this study are available from the corresponding author upon reasonable request.

Field-specific reporting

Please select the best fit for your research. If you are not sure, read the appropriate sections before making your selection.

☒ Life sciences ☐ Behavioural & social sciences ☐ Ecological, evolutionary & environmental sciences

For a reference copy of the document with all sections, see nature.com/authors/policies/ReportingSummary-flat.pdf

Life sciences study design

All studies must disclose on these points even when the disclosure is negative.

Sample size	No sample-size calculation was performed.
Data exclusions	No data was excluded from the analysis.
Replication	All attempts at replication were successful.
Randomization	Samples were allocated randomly into experimental groups.
Blinding	Investigators were blinded for pathology scoring.

Reporting for specific materials, systems and methods

Materials & experimental systems

n/a	Involved in the study
☐	☒ Unique biological materials
☐	☒ Antibodies
☐	☒ Eukaryotic cell lines
☒	☐ Palaeontology
☐	☒ Animals and other organisms
☒	☐ Human research participants

Methods

n/a	Involved in the study
☐	☒ ChIP-seq
☒	☐ Flow cytometry
☒	☐ MRI-based neuroimaging

Unique biological materials

Policy information about availability of materials

Obtaining unique materials	All unique biological materials are readily available from the authors.

Antibodies

Antibodies used	anti-FLAG rabbit antibody F7425 (Sigma); anti-HA rabbit antibody H6908 (Sigma); anti-HilAK90Bu rabbit custom antibody (Thermo Fisher); goat polyclonal anti-rabbit HRP ab97051 (Abcam).
Validation	anti-FLAG rabbit antibody F7425 is validated by Sigma: https://www.sigmaaldrich.com/catalog/product/sigma/f7425 anti-HA rabbit antibody H6908 is validated by Sigma: https://www.sigmaaldrich.com/catalog/product/sigma/h6908 anti-HilAK90Bu rabbit custom antibody is validated throug ELISA by Thermo Fisher.

Eukaryotic cell lines

Policy information about cell lines

Cell line source(s)	HeLa cells and RAW264.7 cells are from ATCC.
Authentication	Each cell line was authenticated by ATCC.
Mycoplasma contamination	All cell lines are tested negative for Mycoplasma.

Commonly misidentified lines (See ICLAC register)	No commonly misidentified lines.

Animals and other organisms

Policy information about studies involving animals; ARRIVE guidelines recommended for reporting animal research

Laboratory animals	Mus musculus C57BL/6J female mice of 7 to 8 weeks old were purchased from the Jackson Laboratory (000664).
Wild animals	The study did not involve wild animals.
Field-collected samples	The study did not involve samples collected from the field.

ChIP-seq

Data deposition

☐ Confirm that both raw and final processed data have been deposited in a public database such as GEO.

☒ Confirm that you have deposited or provided access to graph files (e.g. BED files) for the called peaks.

Data access links *May remain private before publication.*	https://drive.google.com/drive/folders/1XXql01B_7A6OFqR23WPUJv8qZp8PMyL_?usp=sharing
Files in database submission	Stm_14028S_HilA-HA_ChIP1_S13_R1_001 assembled to NC_016856.bai Stm_14028S_HilA-HA_ChIP1_S13_R1_001 assembled to NC_016856.bam Stm_14028S_HilA-HA_ChIP1_S13_R1_001 assembled to NC_016856.fasta Stm_14028S_HilA-HA_ChIP2_S14_R1_001 assembled to NC_016856.bai Stm_14028S_HilA-HA_ChIP2_S14_R1_001 assembled to NC_016856.bam Stm_14028S_HilA-HA_ChIP2_S14_R1_001 assembled to NC_016856.fasta Stm_14028S_HilA-HA_ChIP3_S15_R1_001 assembled to NC_016856.bai Stm_14028S_HilA-HA_ChIP3_S15_R1_001 assembled to NC_016856.bam Stm_14028S_HilA-HA_ChIP3_S15_R1_001 assembled to NC_016856.fasta Stm_14028S_HilAK90KAM-HA_ChIP1_S16_R1_001 assembled to NC_016856.bai Stm_14028S_HilAK90KAM-HA_ChIP1_S16_R1_001 assembled to NC_016856.bam Stm_14028S_HilAK90KAM-HA_ChIP1_S16_R1_001 assembled to NC_016856.fasta Stm_14028S_HilAK90KAM-HA_ChIP2_S17_R1_001 assembled to NC_016856.bai Stm_14028S_HilAK90KAM-HA_ChIP2_S17_R1_001 assembled to NC_016856.bam Stm_14028S_HilAK90KAM-HA_ChIP2_S17_R1_001 assembled to NC_016856.fasta Stm_14028S_HilAK90KAM-HA_ChIP3_S18_R1_001 assembled to NC_016856.bai Stm_14028S_HilAK90KAM-HA_ChIP3_S18_R1_001 assembled to NC_016856.bam Stm_14028S_HilAK90KAM-HA_ChIP3_S18_R1_001 assembled to NC_016856.fasta
Genome browser session (e.g. UCSC)	*Provide a link to an anonymized genome browser session for "Initial submission" and "Revised version" documents only, to enable peer review. Write "no longer applicable" for "Final submission" documents.*

Methodology

Replicates	Each strain was done with 3 biological replicates.
Sequencing depth	Each sample has about 110,000 unique reads mapped to Salmonella genome, each read is 75 bp long and single-read.
Antibodies	Anti-HA tag antibody - ChIP Grade, Abcam, ab9110
Peak calling parameters	Reads were mapped to Salmonella Typhimurium genome (NC_016856) with Bowtie2.
Data quality	Nine peaks are at FDR 5% and 5-fold enrichment.
Software	Genenious 11.0 was used to analyze ChIP-Seq data.